



UNIVERSITY OF LEEDS

This is a repository copy of *Scalable Production of Graphene-Based Wearable E-Textiles*.

White Rose Research Online URL for this paper:

<http://eprints.whiterose.ac.uk/125303/>

Version: Accepted Version

---

**Article:**

Karim, N, Afroj, S, Tan, S et al. (4 more authors) (2017) Scalable Production of Graphene-Based Wearable E-Textiles. *ACS Nano*, 11 (12). pp. 12266-12275. ISSN 1936-0851

<https://doi.org/10.1021/acsnano.7b05921>

---

© 2017 American Chemical Society. This document is the Accepted Manuscript version of a Published Work that appeared in final form in *ACS Nano*, copyright © American Chemical Society after peer review and technical editing by the publisher. To access the final edited and published work see <https://doi.org/10.1021/acsnano.7b05921>

**Reuse**

Items deposited in White Rose Research Online are protected by copyright, with all rights reserved unless indicated otherwise. They may be downloaded and/or printed for private study, or other acts as permitted by national copyright laws. The publisher or other rights holders may allow further reproduction and re-use of the full text version. This is indicated by the licence information on the White Rose Research Online record for the item.

**Takedown**

If you consider content in White Rose Research Online to be in breach of UK law, please notify us by emailing [eprints@whiterose.ac.uk](mailto:eprints@whiterose.ac.uk) including the URL of the record and the reason for the withdrawal request.



[eprints@whiterose.ac.uk](mailto:eprints@whiterose.ac.uk)  
<https://eprints.whiterose.ac.uk/>

# Scalable Production of Graphene-Based Wearable E-Textiles

*‡Nazmul Karim,<sup>1\*</sup> ‡Shaila Afroj,<sup>1,2</sup> Sirui Tan,<sup>3</sup> Pei He,<sup>3</sup> Anura Fernando,<sup>3</sup> Chris Carr,<sup>4</sup>  
and Kostya S Novoselov<sup>1,2</sup>*

<sup>1</sup>The National Graphene Institute (NGI), The University of Manchester, Booth Street East,  
Manchester, M13 9PL, UK

<sup>2</sup>School of Physics & Astronomy, The University of Manchester, Oxford Road, Manchester,  
M13 9PL, UK

<sup>3</sup>School of Materials, The University of Manchester, Oxford Road, Manchester, M13 9PL,  
UK

<sup>4</sup>School of Design, The University of Leeds, Leeds, LS2 9JT,

\* Corresponding author: [mdnazmul.karim@manchester.ac.uk](mailto:mdnazmul.karim@manchester.ac.uk);

**ABSTRACT**

Graphene-based wearable e-textiles are considered to be promising due to their advantages over traditional metal-based technology. However the manufacturing process is complex and currently not suitable for industrial scale application. Here we report a simple, scalable and cost-effective method of producing graphene-based wearable e-textiles through the chemical reduction GO to make stable rGO dispersions which can then be applied to the textile fabric using a simple pad-dry technique. This application method allows the potential manufacture of conductive graphene e-textiles at commercial production rates of ~150 m/min. The graphene e-textile materials produced are durable and washable with acceptable softness/hand feel. The rGO coating enhanced the tensile strength of cotton fabric by ~60% and also the flexibility due to the increase in strain% at maximum load. We demonstrate the potential application of these graphene e-textiles for wearable textiles with activity monitoring sensors. This could potentially lead to a multifunctional single graphene e-textiles garment that can act both as sensors and flexible heating elements powered by the energy stored in graphene textile supercapacitors.

**KEYWORDS:** graphene, wearables, e-textiles, textile sensors and activity monitoring

1  
2  
3 Multi-functional wearable e-textiles are becoming increasingly very popular since such  
4 technology makes life safer, healthier and more comfortable.<sup>1</sup> This technology allows the  
5 production of highly innovative and intelligent e-textile garments that can perform as a  
6 sensor, actuator, power generator and energy storage device all at the same time.<sup>2</sup> The market  
7 for such e-textiles has been growing rapidly and is forecasted to grow up to USD 5 Bn by  
8 2027 through the integration of light weight and flexible electronics into everyday garment.<sup>3</sup>  
9 However, the challenge to achieving this goal lies within the complex and time consuming  
10 manufacturing process of e-textiles and the use of expensive,<sup>4</sup> toxic<sup>5</sup> and non-biodegradable,<sup>6</sup>  
11 not very stable metallic conductive materials such as silver (Ag) and copper (Cu).  
12  
13  
14  
15  
16  
17  
18  
19  
20  
21  
22

23 Graphene has opened up a wide range of flexible electronics applications due to its  
24 outstanding electrical, mechanical and other performance properties.<sup>7-9</sup> The unique properties  
25 of graphene are mostly associated with the individual sheets.<sup>7</sup> Therefore, it is important for  
26 industrial applications that bulk amounts of graphene can be produced in a processable form  
27 that does not agglomerate. However, graphene sheets, unless well separated from each other,  
28 have a tendency to agglomerate and even restack to form graphite through Van der Waals  
29 interactions.<sup>10</sup> The graphite oxide route is currently the most popular wet chemical method  
30 for producing scalable quantities of graphene materials such as graphene oxide (GO)<sup>11</sup> and  
31 reduced graphene oxide (rGO).<sup>12</sup> This is because of its higher yield, good colloidal stability  
32 and excellent dispersibility in various solvents.<sup>13-15</sup>  
33  
34  
35  
36  
37  
38  
39  
40  
41  
42  
43  
44

45 Graphene-based materials, such as graphene oxide (GO) and reduced graphene oxide (rGO),  
46 have already shown great promise by being fabricated into environmental friendly wearable  
47 e-textiles.<sup>16-21</sup> The presence of the negative charge in GO not only helps to form stable  
48 dispersions<sup>14</sup> but also allows their interaction with the functional groups of the  
49 fibres/fabrics.<sup>20, 22</sup> Thus it provides better fixation with textile fabrics and produce flexible,  
50 washable and durable wearable e-textiles. Several techniques have been used to coat textiles  
51  
52  
53  
54  
55  
56  
57  
58  
59  
60

1  
2  
3 with graphene materials such as dip coating,<sup>23</sup> vacuum filtration,<sup>24</sup> brush coating,<sup>25</sup> direct  
4 electrochemical deposition,<sup>26</sup> electrophoresis,<sup>27</sup> kinetic trapping method,<sup>28</sup> wet transfer of  
5 monolayer<sup>29</sup> or screen printing.<sup>30</sup> However, these are time consuming and multi-stage  
6 manufacturing processes; not suitable for large scale production. Therefore, there is a need  
7 for a low-cost, continuous and scalable process for fabricating commercial wearable e-  
8 textiles.

9  
10  
11 The traditional method of coating textiles with rGO usually goes *via* coating textiles with GO  
12 first followed with subsequent reduction by partial restoration of the  $sp^2$  structure.<sup>31</sup> This can  
13 be achieved by chemical,<sup>23</sup> thermal<sup>32</sup> or electrochemical reduction<sup>17</sup> methods. Thermal  
14 reduction of GO coated textiles has also been reported;<sup>19</sup> however the textile fabrics are  
15 temperature sensitive and lose strength significantly at higher temperature.<sup>33</sup> The  
16 electrochemical reduction requires conductive substrates to carry current flow, which is  
17 suitable for carbon cloths only. The majority of graphene e-textiles studies concentrate on  
18 chemical reductants such as ascorbic acid,<sup>18</sup> hydrazine,<sup>27</sup> hydroiodic acid,<sup>34</sup> and sodium  
19 borohydride<sup>23</sup> and sodium hydrosulphite<sup>22</sup> in the post-treatment process, where GO coated  
20 fabrics are reduced to electrically conductive rGO e-textiles. However, most of these  
21 reducing agents are toxic and may not be suitable for e-textiles application which would be in  
22 contact with human body. The other potential reducing agents are either not very efficient or  
23 require longer processing time to reduce the GO.<sup>35</sup> Recently, Shateri-Khalilabad *et al*<sup>23</sup>  
24 reported using of  $Na_2S_2O_4$  as an efficient reducing agent to reduce GO coated textiles.  
25 However, their process involves multiple “dip and dry” coating with GO and post-reduction  
26 with  $Na_2S_2O_4$ , which is time consuming and require a number of cleaning steps. Therefore, it  
27 is desirable to have an efficient and scalable reduction process for manufacturing rGO-based  
28 wearable e-textiles.

1  
2  
3 Here we report a simple, scalable and cost-effective method of producing graphene-based e-  
4 textiles. In contrast with previous approaches, we reduce GO in solution, chemically  
5 functionalise it and use the resulting functionalised rGO to coat the textiles. As illustrated in  
6  
7 Figure 1, we use a modified Hummers method first to synthesize GO and then chemically  
8  
9 reduce this *in-situ* using  $\text{Na}_2\text{S}_2\text{O}_4$ , an efficient and commercially available reducing agent for  
10  
11 textile materials. During *in-situ* chemical reduction of GO, we also incorporate poly (styrene  
12  
13 sulfonate) (PSS) in order to functionalize the surface of rGO to form a stable dispersion. We  
14  
15 use this rGO dispersion to coat textile fabrics using a simple pad-dry continuous process and  
16  
17 subsequently also demonstrate the application of these graphene e-textiles *via* associated  
18  
19 activity monitoring sensors.  
20  
21  
22  
23  
24

## 25 RESULTS AND DISCUSSION

### 26 Scalable Production of Stable rGO Dispersions and Characterisation

27  
28 We synthesized GO using a simple and cheap solution process *i.e.* a modified Hummers  
29  
30 method.<sup>36, 37</sup> In this process, the oxidative intercalation and production of oxygen-containing  
31  
32 functional groups on the graphene layers helps to disperse and stabilise GO sheet in an  
33  
34 aqueous medium.<sup>38</sup> As prepared GO was chemically reduced to rGO using sodium  
35  
36 hydrosulphite ( $\text{Na}_2\text{S}_2\text{O}_4$ ) as the reducing agent.  $\text{Na}_2\text{S}_2\text{O}_4$  is a widely used in the textile  
37  
38 industry for efficient, reliable and rapid reduction of vat dyes in order to solubilise the  
39  
40 pigment molecule.<sup>39</sup> The structure of GO is similar to that of vat dyes used in the textile  
41  
42 industry (Figure S1, Supporting information 2), as oxygen functional groups are covalently  
43  
44 attached to their aromatic benzene rings.<sup>40</sup> With the addition of  $\text{Na}_2\text{S}_2\text{O}_4$  to the yellow-brown  
45  
46 dispersion of GO, the colour of the dispersion turns opaque black almost immediately (Figure  
47  
48 S2, Supporting information), which confirms the efficient reduction of GO. This is in  
49  
50 agreement with previous studies,<sup>40, 41</sup> where a change of colour was observed within 15-20  
51  
52  
53  
54  
55  
56  
57  
58  
59  
60

1  
2  
3 minutes. As dye reduction with  $\text{Na}_2\text{S}_2\text{O}_4$  has already been commercially used for many years  
4  
5 in the textile industry, we therefore believe it has significant commercial potential to be used  
6  
7 for stable graphene dispersions production.  
8

9  
10 Shateri-Khalilabad *et al*<sup>23</sup> used a number of reducing agents such as  $\text{NaBH}_4$ ,  $\text{N}_2\text{H}_4$ ,  $\text{C}_6\text{H}_8\text{O}_6$ ,  
11  
12  $\text{Na}_2\text{S}_2\text{O}_4$  and  $\text{NaOH}$  to reduce GO coated fabrics. However, they found that  $\text{Na}_2\text{S}_2\text{O}_4$  was the  
13  
14 best reducing agent to achieve higher electrical conductivity in the e-textiles. Zhou *et al*<sup>40</sup>  
15  
16 explained the reduction mechanism of  $\text{Na}_2\text{S}_2\text{O}_4$  which has a low electrode potential ( $E^\circ \text{SO}_3^{2-}$   
17  
18  $/\text{S}_2\text{O}_4^{2-} = -1.12 \text{ V}$ ) in alkaline condition and dissociates two protons to become a nucleophile.  
19  
20 This nucleophile attacks the epoxide and hydroxyl groups of GO with a back side  $\text{S}_{\text{N}}2$   
21  
22 nucleophilic reaction to form an intermediate. Reduced graphene oxide is formed due to  
23  
24 hydro-thermal reduction and the reducing agent ( $\text{S}_2\text{O}_4^{2-}$ ) is oxidised to sulphite ( $\text{SO}_3^{2-}$ ).  
25  
26

27  
28 Although the reduction of graphene oxide is a popular approach, the major problem  
29  
30 associated with this route is that rGO aggregates in aqueous solution due to its hydrophobic  
31  
32 nature, especially at higher concentration. To prevent restacking of graphene flakes, surface  
33  
34 characteristics should be modified by the addition of surface functionality through either  
35  
36 covalent bonding or non-covalent interactions.<sup>42, 43</sup> Covalent bonding is commonly preferred  
37  
38 when stability and strong mechanical properties of modified graphene are required. In this  
39  
40 study, we functionalised the rGO surface using poly (styrene sulfonate) (PSS), which  
41  
42 improved the dispersibility and stability of the rGO in aqueous media.<sup>44</sup> The dispersion (3.2  
43  
44 mg/mL) was stable for more than six months and moreover, the PSS functionalised graphene  
45  
46 dispersion offers better wettability<sup>45</sup> and enable better adhesion to the fibrous substrates.  
47  
48  
49

50  
51  
52 Field Emission Gun Scanning Electron Microscopy (FEGSEM) was used to assess the lateral  
53  
54 size of precursor GO and resultant rGO composite ink. Figure 2a shows a statistical analysis  
55  
56 of 100 flakes where the mean lateral dimension of GO was  $5.85 \mu\text{m}$  and that of rGO was  $4.86$   
57  
58

1  
2  
3  $\mu\text{m}$ . The decreased flake size of GO after reduction may be due to the stresses it was subjected  
4 to during pre-mixing and centrifugation steps during post washing cycles. Figure 2b shows  
5 flake thickness ( $h$ ) of GO and rGO, which was 2.07 nm for GO and 2.21 nm for rGO. Figure  
6  
7  
8  
9  
10  
11  
12  
13  
14  
15  
16  
17  
18  
19  
20  
21  
22  
23  
24  
25  
26  
27  
28  
29  
30  
31  
32  
33  
34  
35  
36  
37  
38  
39  
40  
41  
42  
43  
44  
45  
46  
47  
48  
49  
50  
51  
52  
53  
54  
55  
56  
57  
58  
59  
60

2c indicates that the distribution was shifted towards higher  $h$  for rGO, which may be due to the presence of cross-linking polymer (PSS) covering the graphene flake.<sup>44</sup>

XPS analysis provided further evidence of efficient reduction by  $\text{Na}_2\text{S}_2\text{O}_4$ , Figure 2c, as the wide scan XPS spectrum showed a significant increase in carbon content after reduction. The C/O ratio was also increased from 2.4 (GO) to 6.6 (rGO) after reduction, Table 1. Moreover the C(1s) spectra of GO and rGO (Figure S3, Supporting information 4) demonstrated that the peaks associated with oxygen functional groups<sup>46</sup> sharply diminished after GO reduction to rGO, with a small amount of residual oxygen functionality evident at 286.5 eV. The C(1s) spectrum of rGO was almost identical to graphite or graphene, which exhibited clear restoration of graphitic structure through chemical reduction.<sup>47</sup> Figure 2d shows the Raman spectra of GO and rGO which display characteristic D and G peaks. After reduction the intensity ratio of D to G band ( $I_D/I_G$ ) was increased from 0.98 for GO to 1.61 for rGO.

### Scalable Production of Graphene E-textiles

Padding is the most commonly used method in the textile industry to apply functional (*e.g.* water repellent, wrinkle free, moisture management *etc.*) or soft finishes onto textiles. The production speed of pad-dry unit is high and can potentially process approximately 150 m fabric in just one minute. In this study, a laboratory scale pad-dry unit was used to mimic an industrial pad-dry unit, which could potentially be used for large scale industrial production of graphene e-textiles. Figure 3 (a, d) shows a white cotton control fabric which has been desized, scoured and bleached to remove natural and added impurities and colours.<sup>48</sup> As

1  
2  
3 shown in Figure 3a, this control fabric was passed through the padding bath which contains  
4 the rGO dispersion (3.2 mg/mL) and the mangle nip rollers squeeze any excess rGO from the  
5 fabric surface, thus producing a uniform treatment. Almost immediately after coating (within  
6 few seconds), the white cotton fabrics turns black as shown, Figure 3b, due to the uniform  
7 deposition of rGO on the surface (Figure 3h) and also within each individual fibre. The rGO  
8 coated fabric was dried at 100 °C for 5 minutes in a Mathis laboratory dryer to dry off the  
9 water/solvent and fix the graphene onto the textiles.  
10  
11  
12  
13  
14  
15  
16  
17

18 Figure 3d and 3e shows untreated and rGO padded (5 pass) cotton fabrics respectively.  
19 Figure 3f demonstrates the excellent bendability and flexibility of the rGO padded cotton  
20 fabrics, which is similar to untreated cotton fabrics. The rGO coating on cotton fabric hasn't  
21 altered the "drape" (the way a fabric hangs under its own weight) of the fabrics. SEM images  
22 of the untreated cotton fabric, Figure 3g, shows a typically smooth fibre, which clearly  
23 changed the morphology after deposition of the rGO flakes on the cotton fibre surface, Figure  
24 3h. Unlike in the previously reported study where rGO was deposited between the fibres,<sup>19</sup> in  
25 this study the rGO forms a uniform coating around the fibres. This is may be due to the  
26 smooth coating by padding and the hydrogen bonding between residual hydroxyl groups of  
27 rGO and cotton fibres.<sup>20, 21</sup> Therefore, rGO coated fabrics provide electric conductivity  
28 without compromising the breathability, flexibility and comfort of the wearable e-textiles.  
29 Figure 3h also shows some inter-fibre bonding between adjacent fibres, which may be due to  
30 the presence of the PSS cross-linker in the rGO dispersion. Figure 3i shows SEM images of  
31 washed (5 times) rGO coated fabric, which appear almost unchanged even after the repeated  
32 washing cycles.  
33  
34  
35  
36  
37  
38  
39  
40  
41  
42  
43  
44  
45  
46  
47  
48  
49  
50

51 XPS analysis of the untreated and rGO coated cotton fabrics provided further evidence of  
52 efficient coating of rGO on the cotton fibres, Figure 4 (c, d) and Table 1. The wide scan XPS  
53 analysis showed an increase in carbon content from 73.9% for untreated cotton to 82.4% for  
54  
55  
56  
57  
58  
59  
60

1  
2  
3 rGO coated cotton (1 pass) and a decrease in oxygen content from 26.1% for untreated cotton  
4 to 17.6% rGO coated cotton (1 padding pass), Table 1. Moreover, the C/O ratio increased  
5 from 2.8 for untreated cotton to 4.7 for treated cotton (1 padding pass). In addition, with the  
6 increase of number of padding passes, the C/O ratio increased to 6.1 (for 5 padding pass).  
7 This was clearly due to the presence of more rGO flakes on the fibre surface at the higher  
8 number of padding passes. The C (1s) spectrum of untreated cotton fabric in Figure 4c  
9 showed three main peaks that can be fitted into three components arising from C-C bond  
10 (~284.6 eV), C-O groups (hydroxyl, ~286.2 eV) and C=O groups (carbonyl, ~288 eV).<sup>49</sup>  
11 After coating with rGO, the peaks associated with the oxygen functional groups significantly  
12 diminished with small amount of residual oxygen functional groups left around 287.5 eV,  
13 Figure 4d.

14  
15  
16  
17  
18  
19  
20  
21  
22  
23  
24  
25  
26  
27  
28  
29  
30  
31  
32  
33  
34  
35  
36  
37  
38  
39  
40  
41  
42  
43  
44  
45  
46  
47  
48  
49  
50  
51  
52  
53  
54  
55  
56  
57  
58  
59  
60

Figure 4a shows the changes of sheet resistance of the rGO coated fabric with the number of padding passes. After one padding pass with rGO, the sheet resistance of coated fabric is 361.82 k $\Omega$ /sq. There is a slight change in the sheet resistance of rGO coated cotton fabric up to 2 padding cycles. However the sheet resistance then decreased sharply by ~50-60% for each padding pass up to 5 padding passes. The sheet resistance of the rGO coated fabric decreased by ~90% from 348.34 k $\Omega$ /sq (after 2 padding pass) to 36.94 k $\Omega$ /sq (after 5 padding pass). This could possibly be explained by an absorption and adsorption phenomena, where absorption of rGO dispersion into the fibres is predominant in first few padding passes. Once it reached the saturation point, it is then mainly adsorbed on the fibre surface and formed a continuous conductive film by creating better connections between flakes. Thus the sheet resistance of the fabric decreased by presenting more flakes on fibre surface, Figure 3h, and by the restacking of the flakes through the van der Waal forces applied by the squeeze rollers.

Figure 4b shows the washability of the rGO coated fabric (5 padding passes) after a number of washing cycles (1-10). The simulated standard washing conditions generated mechanical

1  
2  
3 agitation and abrasion of the rGO coated fabric in the washing bath and this altered the  
4  
5 continuity of conductive film on the fabric surfaces, resulting in an increase in sheet  
6  
7 resistance.<sup>19</sup> The sheet resistance of rGO coated fabric increased significantly from 36.94  
8  
9 kΩ/sq to 70.32 kΩ/sq after the first washing cycle probably be due to the removal of unfixed  
10  
11 rGO flakes from the fabric surface. After that, the sheet resistance increased moderately to  
12  
13 139.09 kΩ/sq after 10 washing cycles. We also examined various humidity conditions to  
14  
15 observe its effect on the rGO coated cotton e-textiles; however the complex impedance  
16  
17 spectra (CIS) and I-V curves (Figure S4 (a-b), Supporting information 5) showed that  
18  
19 humidity had no effect on the impedance and resistance of rGO coated textiles, which may be  
20  
21 due to the efficient reduction and hydrophobicity of the rGO.<sup>50</sup> Almost similar graphs, were  
22  
23 observed for rGO coated cotton fabrics (with 5 padding passes) at 11%, 53% and 97%  
24  
25 relative humidity.  
26  
27  
28  
29

30 **Table 1.** Wide scan XPS analysis C/O ratio

Sample	C (%)	O (%)	C/O
GO	70.7	29.4	2.4
rGO	86.8	13.2	6.6
Untreated cotton	73.9	26.1	2.8
rGO coated (padded) cotton (1 pass)	82.4	17.6	4.7
rGO coated (padded) cotton (5 pass)	85.8	14.2	6.1

31  
32  
33  
34  
35  
36  
37  
38  
39  
40  
41  
42  
43  
44  
45 The tensile strength of textile fabrics is one of the most important parameters that determines  
46  
47 the quality and life-time of a garment. Some of the chemical processing of cotton or  
48  
49 cellulosic fibres seem to have significant negative effect on their tensile strength due to the  
50  
51 damage in cellulosic structure.<sup>51</sup> Moreover, the higher curing temperature (above 140 °C) for  
52  
53 longer duration reduced the cotton fabric strength significantly due to the intra-  
54  
55 macromolecular crosslinking and depolymerisation of the cellulose.<sup>33</sup> However, these issues  
56  
57  
58  
59  
60

1  
2  
3 were not addressed in previous studies on graphene-based e-textiles, where the toxic reducing  
4 agents such as hydrazine hydrate<sup>27</sup> and a higher thermal reduction temperature for longer  
5 duration<sup>19</sup> were used in the post-reduction process of GO coated textiles. Nevertheless, the  
6 lower or similar tensile strength achieved with chemical reduction of GO coated textiles was  
7 reported to some extent.<sup>23</sup> In contrast, we use an efficient and commonly used chemical  
8 ( $\text{Na}_2\text{S}_2\text{O}_4$ ) for textiles processing as the reducing agent and the relatively lower temperature  
9 (100 °C) for shorter duration (5 minutes) in our study. Figure 5a shows a significant increase  
10 in the tensile strength in both the warp and weft direction of the rGO coated cotton fabrics by  
11 ~20%-30% after single padding pass, almost similar to pigment dyed cotton fabrics and by  
12 ~60% after 5 padding passes. Similarly, the elongation or Strain% at maximum load  
13 increased with rGO coatings showing enhancement in flexibility (displacement).<sup>52</sup> These  
14 results are in agreement with previous studies, however on rGO-based composites.<sup>53</sup>

15  
16  
17  
18  
19  
20  
21  
22  
23  
24  
25  
26  
27  
28  
29  
30  
31 The Kawabata Evaluation System for Fabrics (KES-F) is an objective measurement system  
32 based on tensile, shear, bending compression and surface analysis instruments that measure 16  
33 mechanical parameters using non-destructive forces similar to those used by a human hand  
34 during typical fabric assessment and can characterise the fabric handle qualities (*e.g.* softness  
35 or stiffness, smoothness *etc.*) perceived by human touch.<sup>54</sup> In this study, the shear rigidity,  $G$   
36 and shear hysteresis,  $2HG5$  of the rGO coated cotton fabrics, Figure 5c and Figure 5d, were  
37 measured and it was found that the shear rigidity decreased after coating with rGO. While in  
38 contrast, the shear rigidity increased for the pigment dyed fabrics due to the introduction of  
39 inter-fibre bonding by the cross-linking binder which resulted in a stiffer and harsher hand  
40 feel.<sup>55</sup> The shear hysteresis at  $5^\circ$ ,  $2HG5$  has previously been identified as the “best” indicator  
41 relating to subjective perception of fabric softness and is a sensitive measure of inter-yarn  
42 friction.<sup>56</sup> If a processing treatment lubricates the fibre/yarn surface, such as a fabric softener,  
43  
44  
45  
46  
47  
48  
49  
50  
51  
52  
53  
54  
55  
56  
57  
58  
59  
60

1  
2  
3 the  $2HG5$  value decreases while if the treatment roughens/degrades the surface  $2HG5$   
4 increases. In this case, the  $2HG5$  value decreased with rGO coating, suggesting there was no  
5 formation of “restricting” interfibre bonds but rather the rGO coating lubricate the fibre  
6 surfaces and resulted in an overall improvement in the fabric softness. In contrast, for  
7 pigment dyed fabric the introduction of inter-fibre bonding in the fabric structure resulted in a  
8 stiffening/harshening of the fabric handle and this was reflected in the much higher  $2HG5$   
9 values observed, Figure 5d.  
10  
11  
12  
13  
14  
15  
16  
17

### 18 **Wearable Sensor Application**

19  
20  
21 Figure 6a shows the changes in resistances per total length of the rGO coated fabric at various  
22 bending positions with concave down at various cord lengths (Figure S8, Supporting  
23 information 7), when the test is carried out on a tensile tester. Here, the cord length is defined  
24 as the distance between the tensile tester grips for the sensor material, under investigation. As  
25 seen in Figure 6a, a repeatable response in forward (bending) and reverse (bending back)  
26 directions was observed.<sup>57</sup> Similarly for compression with concave upward position, the  
27 change in resistance of the rGO coated cotton fabrics was repeatable in both the forward  
28 (compression) and reverse (compression back) directions, Figure 6b. Unlike in other studies,  
29 where the change in resistance of the coated or printed fabrics with bending (increase) and  
30 compression (decrease) was the opposite,<sup>19, 58</sup> here in both cases the resistance of the rGO  
31 coated fabric increased with the increase of cord length for bending and compression. This  
32 may be due to the fact that individual cotton fibres were uniformly coated with rGO during  
33 padding on both sides of the fabric, and still maintained the same porosity of cotton woven  
34 fabric. Moreover, strong connectivity between the flakes was achieved due to the pressure  
35 applied by padding rollers. Thus produced rGO coated fabric would provide better comfort  
36 and breathability to users. However, the change in resistance ( $\Delta R/R_0$ ) varied during bending  
37 and compression may be due to the different structure on face and back side of the fabric.  
38  
39  
40  
41  
42  
43  
44  
45  
46  
47  
48  
49  
50  
51  
52  
53  
54  
55  
56  
57  
58  
59  
60

1  
2  
3 In order to investigate the suitability of the rGO coated fabrics to be used as an activity  
4 monitoring sensor, for example wrist movement monitoring, a piece of rGO coated (5  
5 padding passes) fabric was mounted on a wrist joint, Figure 6c (1-2) and the change in  
6 resistance per 8 cm length of the rGO coated fabric was continuously recorded during the  
7 wrist movement. Therefore, when the sensor is mounted on the wrist and the sensor material  
8 on the wrist is bent and unbent cyclically. The sensory resistance data collected from the  
9 wrist mounted sensor is shown in Figure 6c and 6d. Figure 6d shows the change in resistance  
10 due to the upward and downward movement of the wrist joint for a selected section of the  
11 total wrist activity recorded. The results show the capability of the rGO coated fabric to  
12 capture mechanical events such as bending/unbending, stretching/relaxation and  
13 twisting/untwisting. The woven cotton fabric showed the least variation in the electrical  
14 resistance over long period of cyclic tensile tests. Figure S11 (a-b) shows that the woven  
15 cotton twill fabric has different appearance on their face and back side of the fabric  
16 (Supporting information 8). This imbalance in the surface structure caused the surface stress  
17 distributions on each side to vary. The strain% of cotton fabric at the elastic limit is 2%.  
18 Therefore, in order to ensure the least amount of plastic deformation of the fibre structure, the  
19 electromechanical performance of these fabrics were investigated within each respective  
20 elastic limits.

## 21 22 23 24 25 26 27 28 29 30 31 32 33 34 35 36 37 38 39 40 41 42 **CONCLUSIONS**

43  
44  
45 We report a simple and scalable production method for rGO dispersions and the coating of  
46 cotton textile fabrics with the rGO dispersions in order to produce electrically conductive  
47 graphene e-textiles. The rGO coated fabrics thus produced are washable, flexible and  
48 bendable and exhibits a significant increase in the fabric tensile strength (by ~60%) and  
49 strain%. We also demonstrate the suitability of rGO coated fabric for applications as strain  
50 sensors to monitor human activities. We believe our scalable production method of producing  
51  
52  
53  
54  
55  
56  
57  
58  
59  
60

1  
2  
3 graphene-based wearable e-textiles is an important step towards moving from R&D-based e-  
4  
5 textiles to actual real world applications.  
6  
7

## 8 **EXPERIMENTAL METHODS**

### 9 **Materials**

10  
11  
12 Flake graphite (Grade 3061) was supplied by Asbury Graphite Mills, USA. Poly(sodium 4-  
13 styrene sulfonate) (PSS,  $M_w \sim 70,000$ , powder), sodium hydrosulphite (~82%), ammonia,  
14  
15 potassium permanganate ( $KMnO_4$ ), sulfuric acid ( $H_2SO_4$ , ~99%), hydrogen peroxide ( $H_2O_2$ ,  
16  
17 ~30%) were purchased from Sigma-Aldrich, UK and used as received. 100% cotton 3/1 Twill  
18  
19 fabrics were manufactured internally in the University of Manchester weaving laboratory and  
20  
21 desized, scoured and bleached.  
22  
23  
24  
25

### 26 **Synthesis of GO and rGO**

27  
28  
29 Graphene oxide (GO) was prepared using a modified Hummers method as described  
30 elsewhere.<sup>37</sup> A brown dispersion of GO (1 mg/mL) was prepared by adding 160 mg GO to  
31  
32 160 mL of deionized (DI) water and sonicated for 30 min. In order to form a stable  
33  
34 dispersion, 1.6 gm PSS was mixed into the GO dispersion by vigorous stirring. The resulting  
35  
36 suspension was transferred to a round-bottom flask placed in an oil bath.  $Na_2S_2O_4$  (1.2 gm)  
37  
38 and  $NH_3$  (required to adjust pH 9-10) were added to the dispersion with vigorous stirring.  
39  
40 This mixture was held at 90 °C for 12 hours under closed conditions in order to obtain a  
41  
42 black dispersion. Any residual  $Na_2S_2O_4$  and PSS was washed from the rGO by washing  
43  
44 several times with deionised water to remove any residues present and finally diluted into  
45  
46 distilled water (DI) to adjust the rGO dispersion concentration to 3.2 mg/mL.  
47  
48  
49  
50  
51  
52  
53  
54  
55  
56  
57  
58  
59  
60

### Continuous Pad-drying of Textiles with rGO Ink

Textile fabrics were padded one dip and one nip through rGO dispersions to a wet pick-up of ~80% on the weight of the fabric (o.w.f.). The wet pick-up% was calculated using following formula:

$$\text{Pick-up}\% = \frac{(\text{The weight of rGO coated fabric} - \text{the dry weight of untreated fabric})}{\text{The dry weight of untreated fabric}} \times 100\% \dots\dots\dots (1)$$

The rGO padded fabrics were subsequently dried at 100 °C for 10 minutes and were studied for e-textiles application. Also, several rGO coated samples were prepared using multiple (1 to 10) padding passes to establish any improvement in the electrical conductivity of rGO coated fabrics. In order to asses with comparable textiles, a pigment dyed cotton fabric sample was also prepared using a standard textile pigment dyeing recipe for 3% pigment black shade (recipe in supporting information Table 1). The same padding method and parameters were used to apply pigments on the similar fabrics used for e-textiles.

### Washability and Humidity Testing

The washability of the rGO coated cotton fabrics was assessed according to BS EN ISO 105 C06 A1S, by treating rGO coated fabrics in a solution containing 4 g/L ECE reference Detergent B and 10 stainless steel balls at 40 °C for 30 minutes. 10 steel balls were used to simulate the agitation and abrasion that a garment is subject to during a standard washing cycle. The fabrics were rinsed subsequently in running water at ambient temperature and air dried at room temperature prior to further analysis.

The influence of humidity was measured by exposing the sample to a range off controlled relative humidity (RH) levels, 11%, 53%, and 97%. To produce different RH environments, saturated aqueous solutions of LiCl, and K<sub>2</sub>SO<sub>4</sub> were prepared (Sigma-Aldrich) and placed in airtight glass vessels at a temperature of 24 °C, which yielded atmospheres with RHs of 11%,

1  
2  
3 and 97%, respectively. The 53%RH is the room RH level. The complex impedance spectra  
4 (CIS) and I-V data of the sample was measured using a Portable Electrochemical Interface &  
5 Impedance Analyser (Ivium Technologies B.V., Eindhoven, Netherlands).  
6  
7  
8  
9

### 10 **Materials Characterisation**

11  
12  
13 The sheet resistance of the conductive e-textiles was measured in Van Der Pouw geometry (a  
14 factor of 4.532 was used to obtain the sheet resistance from the raw measurements) using a  
15 Jandel four-probe system (Jandel Engineering Ltd, Leighton, UK). The mean sheet resistance  
16 was calculated from the average of six measurements. A Zeiss Ultra Scanning Electron  
17 Microscope (SEM) was used to analyse the surface topography of the untreated and rGO  
18 coated fabrics and also the flake size of GO and rGO. The dispersions were diluted 1000  
19 times and drop-casted on Si/SiO<sub>2</sub> (290 nm oxide on plain silicon) for each sample, images  
20 were taken at 10 different locations on the sample. A Dimension Icon (Bruker) Atomic Force  
21 Microscopy (AFM) was used to determine GO and rGO flake thickness. A Renishaw Raman  
22 System equipped with 633 nm laser was used to collect Raman spectra of GO and rGO  
23 flakes. A Kratos Axis X-ray Photoelectron Spectroscopy (XPS) system was used to  
24 characterise the surface of untreated and rGO coated textiles and also the GO and rGO flakes.  
25  
26  
27  
28  
29  
30  
31  
32  
33  
34  
35  
36  
37  
38  
39  
40 Tensile strength and strain% of untreated, rGO coated and pigment dyed cotton fabrics  
41 (5×2.5 cm) were measured by a Zwick/Roell Tensile Tester (Zwick Roell Group, Germany)  
42 at 200 mm/min speed, and calculated as average from three measurements in both warp and  
43 weft directions of the fabrics. The Kawabata Evaluation System for Fabrics (KES-F) was  
44 used to determine the mechanical and surface properties of untreated and rGO coated (5  
45 padding passes) fabric.<sup>54</sup> The samples (20×20 cm) were conditioned for 24 h at 20 °C and 65  
46  
47  
48  
49  
50  
51  
52  
53  
54  
55  
56  
57  
58  
59  
60

1  
2  
3 We used various cord lengths (Figure S8-10, Supplementary Information) during bending  
4 (concave down) and compression (concave upward) to measure the change of resistance of  
5 rGO coated fabrics (8×1.5 cm). The cord length of the rGO coated fabric was controlled on a  
6  
7 Zwick/Roell Tensile Tester (Zwick Roell Group, Germany) during bending and compression  
8  
9 test both in the forward and reverse direction. The change of sheet resistance with the change  
10  
11 of cord lengths of rGO coated fabric (8×1.5 cm) during bending and compression was  
12  
13 captured using a National Instrument 9219 data acquisition card (NI, American). A piece of  
14  
15 rGO coated (5 pass) fabric (8×1.5 cm) was also mounted on a wrist joint and the changes in  
16  
17 resistance of the rGO coated fabrics due to upward and downward movement were measured  
18  
19 using a National Instrument 9219 card (NI, American).  
20  
21  
22  
23  
24

## 25 **ASSOCIATED CONTENT**

### 26 **Supporting Information**

27  
28  
29  
30 Supporting information contains the formulation (recipe) for pigment dyeing; the chemical  
31  
32 structures of the vat dyes and sodium hydrosulphite ( $\text{Na}_2\text{S}_2\text{O}_4$ ); images to show the efficient  
33  
34 reduction of GO using  $\text{Na}_2\text{S}_2\text{O}_4$ ; High resolution XPS spectra of GO and rGO; the effect of  
35  
36 humidity on the rGO coated textiles; SEM images of untreated, rGO coated and washed rGO  
37  
38 coated cotton fabrics, cord lengths, the change of resistance with bending and compression  
39  
40 and the face and reverse side appearance of coated cotton fabrics. A video is also added as the  
41  
42 supporting information to demonstrate the capability of rGO coated fabric to capture  
43  
44 mechanical events such as the resistance change during upward and downward movement of  
45  
46 wrist. The supporting information is available free of charge *via* the Internet at  
47  
48 <http://pubs.acs.org>.  
49  
50  
51  
52  
53  
54  
55  
56  
57  
58  
59  
60

## AUTHOR INFORMATION

### Corresponding Author

All the correspondence should be addressed to [mdnazmul.karim@manchester.ac.uk](mailto:mdnazmul.karim@manchester.ac.uk)

### Author Contributions

‡ Shaila Afroj and Nazmul Karim contributed equally as joint first author. The manuscript was written through contributions of all authors. All authors have given approval to the final version of the manuscript.

## ACKNOWLEDGMENT

Authors kindly acknowledge the Government of Bangladesh for PhD funding of Shaila Afroj and the National Graphene Institute, the University of Manchester. This work was supported by the EU Graphene Flagship Program, European Research Council Synergy Grant Hetero2D, The Royal Society, Engineering and Physical Sciences Research Council (EPSRC, UK) and US Army Research Office (W911NF-16-1-0279). Authors also kindly acknowledge Dr Ben Spencer, Daniel Wand and Jianguo Qu for the help with XPS, graphics and KES-F, respectively.

## REFERENCES

1. De Rossi, D., Electronic Textiles: A Logical Step. *Nat. Mater.* 2007, 6, 328-329.
2. Service, R. F., Electronic Textiles Charge Ahead. *Science* 2003, 301, 909-911.
3. IDTechEX, E-Textiles 2017-2027: Technologies, Markets, Players. 2017.
4. Xu, L.; Yang, G.; Jing, H.; Wei, J.; Han, Y., Ag-Graphene Hybrid Conductive Ink for Writing Electronics. *Nanotechnology* 2014, 25, 055201.

- 1  
2  
3 5. Sondergaard, R. R.; Espinosa, N.; Jorgensen, M.; Krebs, F. C., Efficient  
4 Decommissioning and Recycling of Polymer Solar Cells: Justification for Use of Silver.  
5  
6 *Energy Environ. Sci.* 2014, 7, 1006-1012.
- 7  
8  
9 6. Irimia-Vladu, M.; Głowacki, E. D.; Voss, G.; Bauer, S.; Sariciftci, N. S., Green and  
10 Biodegradable Electronics. *Mater. Today* 2012, 15, 340-346.
- 11  
12  
13 7. Novoselov, K. S.; Geim, A. K.; Morozov, S. V.; Jiang, D.; Zhang, Y.; Dubonos, S.  
14 V.; Grigorieva, I. V.; Firsov, A. A., Electric Field Effect In Atomically Thin Carbon Films.  
15  
16 *Science* 2004, 306, 666-669.
- 17  
18  
19 8. Geim, A. K., Graphene: Status and Prospects. *Science* 2009, 324, 1530-1534.
- 20  
21  
22 9. He, Q.; Wu, S.; Yin, Z.; Zhang, H., Graphene-Based Electronic Sensors. *Chem. Sci.*  
23  
24 2012, 3, 1764-1772.
- 25  
26  
27 10. Li, D.; Müller, M. B.; Gilje, S.; Kaner, R. B.; Wallace, G. G., Processable Aqueous  
28 Dispersions of Graphene Nanosheets. *Nat. Nanotechnol.* 2008, 3, 101-105.
- 29  
30  
31 11. Stankovich, S.; Dikin, D. A.; Dommett, G. H. B.; Kohlhaas, K. M.; Zimney, E. J.;  
32 Stach, E. A.; Piner, R. D.; Nguyen, S. T.; Ruoff, R. S., Graphene-Based Composite Materials.  
33  
34 *Nature* 2006, 442, 282-286.
- 35  
36  
37 12. Stankovich, S.; Dikin, D. A.; Piner, R. D.; Kohlhaas, K. A.; Kleinhammes, A.; Jia, Y.;  
38 Wu, Y.; Nguyen, S. T.; Ruoff, R. S., Synthesis of Graphene-Based Nanosheets *via* Chemical  
39 Reduction of Exfoliated Graphite Oxide. *Carbon* 2007, 45, 1558-1565.
- 40  
41  
42 13. Kim, J.; Cote, L. J.; Kim, F.; Yuan, W.; Shull, K. R.; Huang, J., Graphene Oxide  
43 Sheets at Interfaces. . *J. Am. Chem. Soc.* 2010, 132, 8180-8186.
- 44  
45  
46  
47 14. Li, D.; Muller, M. B.; Gilje, S.; Kaner, R. B.; Wallace, G. G., Processable Aqueous  
48 Dispersions of Graphene Nanosheets. *Nat. Nanotechnol.* 2008, 3, 101-105.
- 49  
50  
51 15. Paredes, J. I.; Villar-Rodil, S.; Martínez-Alonso, A.; Tascón, J. M. D., Graphene  
52 Oxide Dispersions in Organic Solvents. *Langmuir* 2008, 24, 10560-10564.
- 53  
54  
55  
56  
57  
58  
59  
60

- 1  
2  
3 16. Yu, G.; Hu, L.; Vosgueritchian, M.; Wang, H.; Xie, X.; McDonough, J. R.; Cui, X.;  
4 Cui, Y.; Bao, Z., Solution-Processed Graphene/MnO<sub>2</sub> Nanostructured Textiles for High-  
5 Performance Electrochemical Capacitors. *Nano Lett.* 2011, 11, 2905-2911.  
6  
7  
8  
9 17. Liu, L.; Yu, Y.; Yan, C.; Li, K.; Zheng, Z., Wearable Energy-Dense and Power-Dense  
10 Supercapacitor Yarns Enabled by Scalable Graphene–Metallic Textile Composite Electrodes.  
11 *Nat. Commun.* 2015, 6, 7260.  
12  
13  
14  
15 18. Shateri-Khalilabad, M.; Yazdanshenas, M. E., Preparation of Superhydrophobic  
16 Electroconductive Graphene-Coated Cotton Cellulose. *Cellulose* 2013, 20, 963-972.  
17  
18  
19 19. Ren, J.; Wang, C.; Zhang, X.; Carey, T.; Chen, K.; Yin, Y.; Torrisi, F.,  
20 Environmentally-Friendly Conductive Cotton Fabric as Flexible Strain Sensor Based on Hot  
21 Press Reduced Graphene Oxide. *Carbon* 2017, 111, 622-630.  
22  
23  
24  
25 20. Abdelkader, A. M.; Karim, N.; Vallés, C.; Afroj, S.; Novoselov, K. S.; Yeates, S. G.,  
26 Ultraflexible and Robust Graphene Supercapacitors Printed on Textiles for Wearable  
27 Electronics Applications. *2D Mater.* 2017, 4.  
28  
29  
30  
31 21. Karim, N.; Afroj, S.; Malandraki, A.; Butterworth, S.; Beach, C.; Rigout, M.;  
32 Novoselov, K.; Casson, A. J.; Yeates, S., All Inkjet-Printed Graphene-Based Conductive  
33 Patterns for Wearable E-Textile Applications. *J. Mater. Chem. C.* 2017.  
34  
35  
36  
37 22. Molina, J.; Fernández, J.; Inés, J. C.; del Río, A. I.; Bonastre, J.; Cases, F.,  
38 Electrochemical Characterization of Reduced Graphene Oxide-Coated Polyester Fabrics.  
39 *Electrochim. Acta* 2013, 93, 44-52.  
40  
41  
42  
43 23. Shateri-Khalilabad, M.; Yazdanshenas, M. E., Fabricating Electroconductive Cotton  
44 Textiles Using Graphene. *Carbohydr. Polym.* 2013, 96, 190-195.  
45  
46  
47  
48 24. Tang, X.; Tian, M.; Qu, L.; Zhu, S.; Guo, X.; Han, G.; Sun, K.; Hu, X.; Wang, Y.;  
49 Xu, X., Functionalization of Cotton Fabric With Graphene Oxide Nanosheet and Polyaniline  
50 for Conductive and UV Blocking Properties. *Synth. Met.* 2015, 202, 82-88.  
51  
52  
53  
54  
55  
56  
57  
58  
59  
60

- 1  
2  
3 25. Javed, K.; Galib, C. M. A.; Yang, F.; Chen, C. M.; Wang, C., A New Approach to  
4 Fabricate Graphene Electro-Conductive Networks on Natural Fibers by Ultraviolet Curing  
5 Method. *Synth. Met.* 2014, 193, 41-47.  
6  
7  
8  
9 26. Cao, Y.; Zhu, M.; Li, P.; Zhang, R.; Li, X.; Gong, Q.; Wang, K.; Zhong, M.; Wu, D.;  
10 Lin, F.; Zhu, H., Boosting Supercapacitor Performance of Carbon Fibres Using  
11 Electrochemically Reduced Graphene Oxide Additives. *Phys. Chem. Chem. Phys.* 2013, 15,  
12 19550-19556.  
13  
14  
15  
16  
17 27. Maiti, U. N.; Maiti, S.; Das, N. S.; Chattopadhyay, K. K., Hierarchical Graphene  
18 Nanocones Over 3D Platform of Carbon Fabrics: A Route Towards Fully Foldable Graphene  
19 Based Electron Source. *Nanoscale* 2011, 3, 4135-4141.  
20  
21  
22  
23 28. Woltornist, S. J.; Alamer, F. A.; McDannald, A.; Jain, M.; Sotzing, G. A.; Adamson,  
24 D. H., Preparation of Conductive Graphene/Graphite Infused Fabrics Using an Interface  
25 Trapping Method. *Carbon* 2015, 81, 38-42.  
26  
27  
28  
29 29. Neves, A. I. S.; Bointon, T. H.; Melo, L. V.; Russo, S.; de Schrijver, I.; Craciun, M.  
30 F.; Alves, H., Transparent Conductive Graphene Textile Fibers. *Sci. Rep.* 2015, 5, 9866.  
31  
32  
33 30. Skrzetuska, E.; Puchalski, M.; Krucińska, I., Chemically Driven Printed Textile  
34 Sensors Based on Graphene and Carbon Nanotubes. *Sensors* 2014, 14, 16816.  
35  
36  
37  
38 31. Samad, Y. A.; Li, Y.; Alhassan, S. M.; Liao, K., Non-Destroyable Graphene Cladding  
39 an a Range of Textile and Other Fibers and Fiber Mats. *RSC Adv.* 2014, 4, 16935-16938.  
40  
41  
42  
43 32. Ramadoss, A.; Saravanakumar, B.; Kim, S. J., Thermally Reduced Graphene Oxide-  
44 Coated Fabrics for Flexible Supercapacitors and Self-Powered Systems. *Nano Energy* 2015,  
45 15, 587-597.  
46  
47  
48  
49 33. Xu, W.; Li, Y., Cotton Fabric Strength Loss From Treatment with Polycarboxylic  
50 Acids for Durable Press Performance. *Text. Res. J.* 2000, 70, 957-961.  
51  
52  
53  
54  
55  
56  
57  
58  
59  
60

- 1  
2  
3 34. Ju Yun, Y.; Hong, W. G.; Choi, N. J.; Hoon Kim, B.; Jun, Y.; Lee, H. K.,  
4  
5 Ultrasensitive and Highly Selective Graphene-Based Single Yarn for Use in Wearable Gas  
6  
7 Sensor. *Sci. Rep.* 2015, 5, 10904.  
8
- 9 35. Gao, J.; Liu, F.; Liu, Y.; Ma, N.; Wang, Z.; Zhang, X., Environment-Friendly Method  
10  
11 to Produce Graphene that Employs Vitamin C and Amino Acid. *Chem. Mater.* 2010, 22,  
12  
13 2213-2218.  
14
- 15 36. Hummers, W. S.; Offeman, R. E., Preparation of Graphitic Oxide. *J. Am. Chem. Soc.*  
16  
17 1958, 80, 1339-1339.  
18
- 19 37. Rourke, J. P.; Pandey, P. A.; Moore, J. J.; Bates, M.; Kinloch, I. A.; Young, R. J.;  
20  
21 Wilson, N. R., The Real Graphene Oxide Revealed: Stripping the Oxidative Debris from the  
22  
23 Graphene-Like Sheets. *Angew. Chem.* 2011, 123, 3231-3235.  
24
- 25 38. Zhong, Y. L.; Tian, Z.; Simon, G. P.; Li, D., Scalable Production of Graphene *via* Wet  
26  
27 Chemistry: Progress And Challenges. *Mater. Today* 2015, 18, 73-78.  
28
- 29 39. Yoe, J. H., The Reduction of Certain Vat Dyes By Means of Alkaline Sodium  
30  
31 Hydrosulphite. *J. Phys. Chem.* 1923, 28, 1211-1217.  
32
- 33 40. Tiannan, Z.; Feng, C.; Kai, L.; Hua, D.; Qin, Z.; Jiwen, F.; Qiang, F., A Simple and  
34  
35 Efficient Method to Prepare Graphene by Reduction of Graphite Oxide with Sodium  
36  
37 Hydrosulfite. *Nanotechnology* 2011, 22, 045704.  
38
- 39 41. Zhou, T.; Chen, F.; Tang, C.; Bai, H.; Zhang, Q.; Deng, H.; Fu, Q., The Preparation of  
40  
41 High Performance and Conductive Poly (Vinyl Alcohol)/Graphene Nanocomposite *via*  
42  
43 Reducing Graphite Oxide with Sodium Hydrosulfite. *Compos. Sci. Technol.* 2011, 71, 1266-  
44  
45 1270.  
46
- 47 42. Liu, J.; Tang, J.; Gooding, J. J., Strategies for Chemical Modification of Graphene  
48  
49 and Applications of Chemically Modified Graphene. *J. Mater. Chem.* 2012, 22, 12435-  
50  
51 12452.  
52  
53  
54  
55  
56  
57  
58  
59  
60

- 1  
2  
3 43. Lonkar, S. P.; Deshmukh, Y. S.; Abdala, A. A., Recent Advances in Chemical  
4  
5 Modifications of Graphene. *Nano Res.* 2015, 8, 1039-1074.  
6  
7 44. Stankovich, S.; Piner, R. D.; Chen, X.; Wu, N.; Nguyen, S. T.; Ruoff, R. S., Stable  
8  
9 Aqueous Dispersions of Graphitic Nanoplatelets *via* the Reduction of Exfoliated Graphite  
10  
11 Oxide in the Presence of Poly (Sodium 4-Styrenesulfonate). *J. Mater. Chem.* 2006, 16, 155-  
12  
13 158.  
14  
15 45. Wei, D.; Li, H.; Han, D.; Zhang, Q.; Niu, L.; Yang, H.; Bower, C.; Andrew, P.;  
16  
17 Ryhänen, T., Properties of Graphene Inks Stabilized by Different Functional Groups.  
18  
19 *Nanotechnology* 2011, 22, 245702.  
20  
21 46. Abdelkader, A.; Kinloch, I.; Dryfe, R., High-Yield Electro-Oxidative Preparation of  
22  
23 Graphene Oxide. *Chem. Commun.* 2014, 50, 8402-8404.  
24  
25 47. Wang, T.; Li, Y.; Geng, S.; Zhou, C.; Jia, X.; Yang, F.; Zhang, L.; Ren, X.; Yang, H.,  
26  
27 Preparation of Flexible Reduced Graphene Oxide/Poly(Vinyl Alcohol) Film with Superior  
28  
29 Microwave Absorption Properties. *RSC Adv.* 2015, 5, 88958-88964.  
30  
31 48. Tomasino, C., *Chemistry & Technology of Fabric Preparation & Finishing.* North  
32  
33 Carolina State University North Carolina: 1992.  
34  
35 49. Shang, S. M.; Li, Z.; Xing, Y.; Xin, J. H.; Tao, X. M., Preparation of Durable  
36  
37 Hydrophobic Cellulose Fabric from Water Glass And Mixed Organosilanes. *Appl. Surf. Sci.*  
38  
39 2010, 257, 1495-1499.  
40  
41 50. Su, Y.; Kravets, V. G.; Wong, S. L.; Waters, J.; Geim, A. K.; Nair, R. R.,  
42  
43 Impermeable Barrier Films and Protective Coatings Based on Reduced Graphene Oxide. *Nat.*  
44  
45 *Commun.* 2014, 5, 4843.  
46  
47 51. Powers, D., Effect of Synthetic Resins on Cellulose and Protein Fibers. *Ind. Eng.*  
48  
49 *Chem. Res.* 1945, 37, 188-193.  
50  
51  
52  
53  
54  
55  
56  
57  
58  
59  
60

- 1  
2  
3 52. Liu, Y.; Wang, X.; Qi, K.; Xin, J., Functionalization of Cotton with Carbon  
4 Nanotubes. *J. Mater. Chem.* 2008, 18, 3454-3460.  
5  
6  
7 53. Li, Z.; Guo, Q.; Li, Z.; Fan, G.; Xiong, D. B.; Su, Y.; Zhang, J.; Zhang, D., Enhanced  
8 Mechanical Properties of Graphene (Reduced Graphene Oxide)/Aluminum Composites with  
9 a Bioinspired Nanolaminated Structure. *Nano Lett.* 2015, 15, 8077-8083.  
10  
11  
12  
13 54. Kawabata, S.; Niwa, M., Fabric Performance in Clothing and Clothing Manufacture.  
14 *J. Text. Inst.* 1989, 80, 19-50.  
15  
16  
17 55. Karim, M. N.; Rigout, M.; Yeates, S. G.; Carr, C., Surface Chemical Analysis of the  
18 Effect of Curing Conditions on the Properties of Thermally-Cured Pigment Printed Poly  
19 (Lactic Acid) Fabrics. *Dyes Pigm.* 2014, 103, 168-174.  
20  
21  
22  
23 56. Finnimore, E.; Konig, A., Instrumental Assessment of Softening Effects on Fabrics: I.  
24 Correlation between Instrumental Measurements and Manual Assessments, *Melliand*  
25 *Textilberichte* 1986, 67, 514-516.  
26  
27  
28  
29 57. Cheng, Y.; Wang, R.; Sun, J.; Gao, L., A Stretchable and Highly Sensitive Graphene-  
30 Based Fiber for Sensing Tensile Strain, Bending, and Torsion. *Adv. Mater.* 2015, 27, 7365-  
31 7371.  
32  
33  
34  
35  
36  
37 58. Liao, X.; Liao, Q.; Yan, X.; Liang, Q.; Si, H.; Li, M.; Wu, H.; Cao, S.; Zhang, Y.,  
38 Flexible and Highly Sensitive Strain Sensors Fabricated by Pencil Drawn for Wearable  
39 Monitor. *Adv. Funct. Mater.* 2015, 25, 2395-2401.  
40  
41  
42  
43  
44  
45  
46  
47  
48  
49  
50  
51  
52  
53  
54  
55  
56  
57  
58  
59  
60

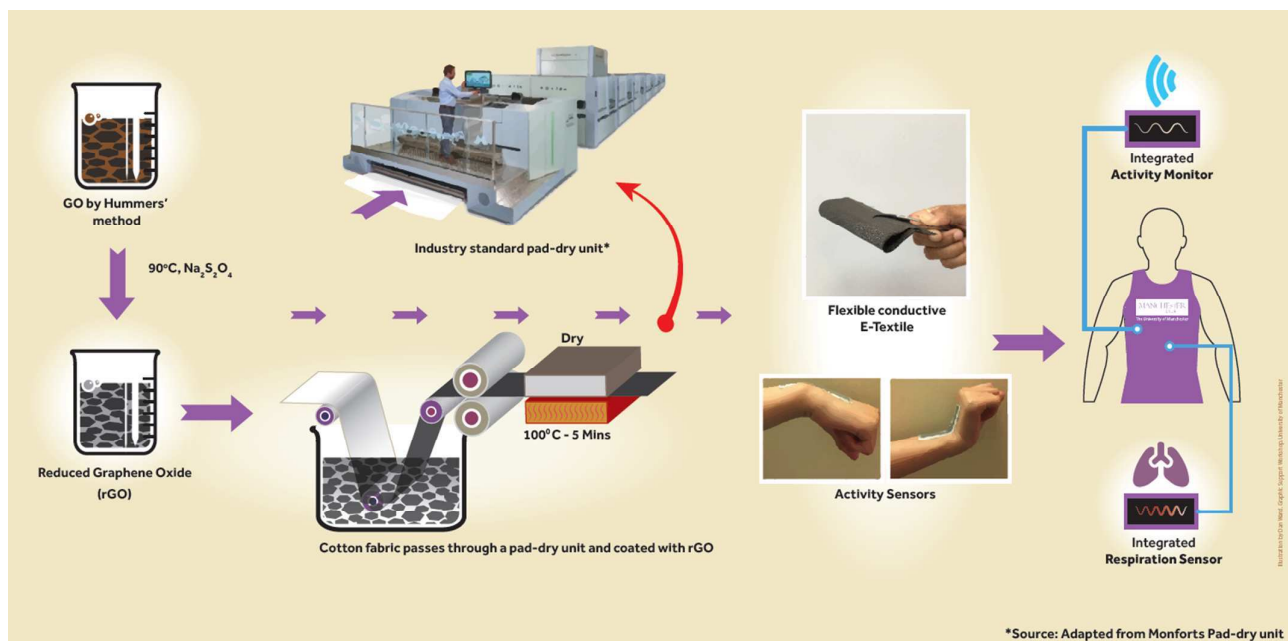


**Figure 1.** Schematic diagram of the scalable production of graphene-based wearable e-textiles. Illustration by Daniel Wand and used with permission from the artist.

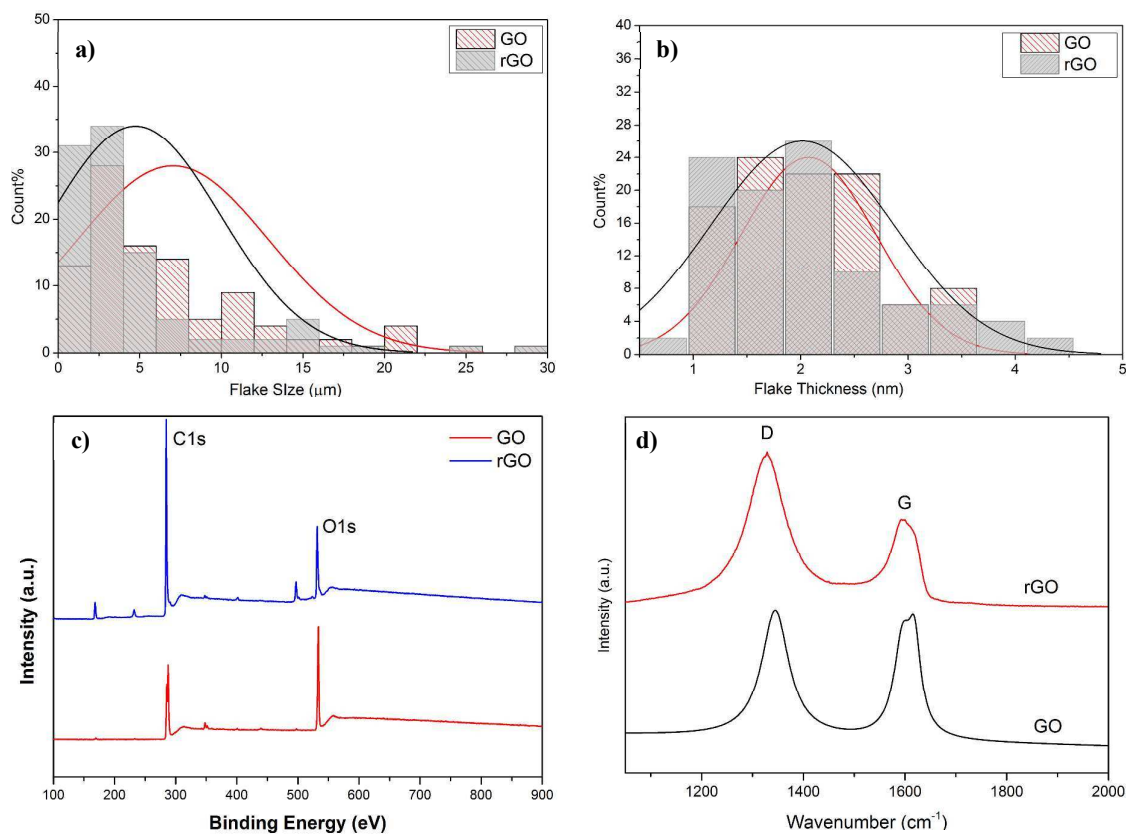


**Figure 2.** a) Flake size distribution of GO and rGO; b) Flake thickness distribution of GO and rGO; c) Wide scan XPS spectra of GO and rGO and d) Raman spectra of GO and rGO.

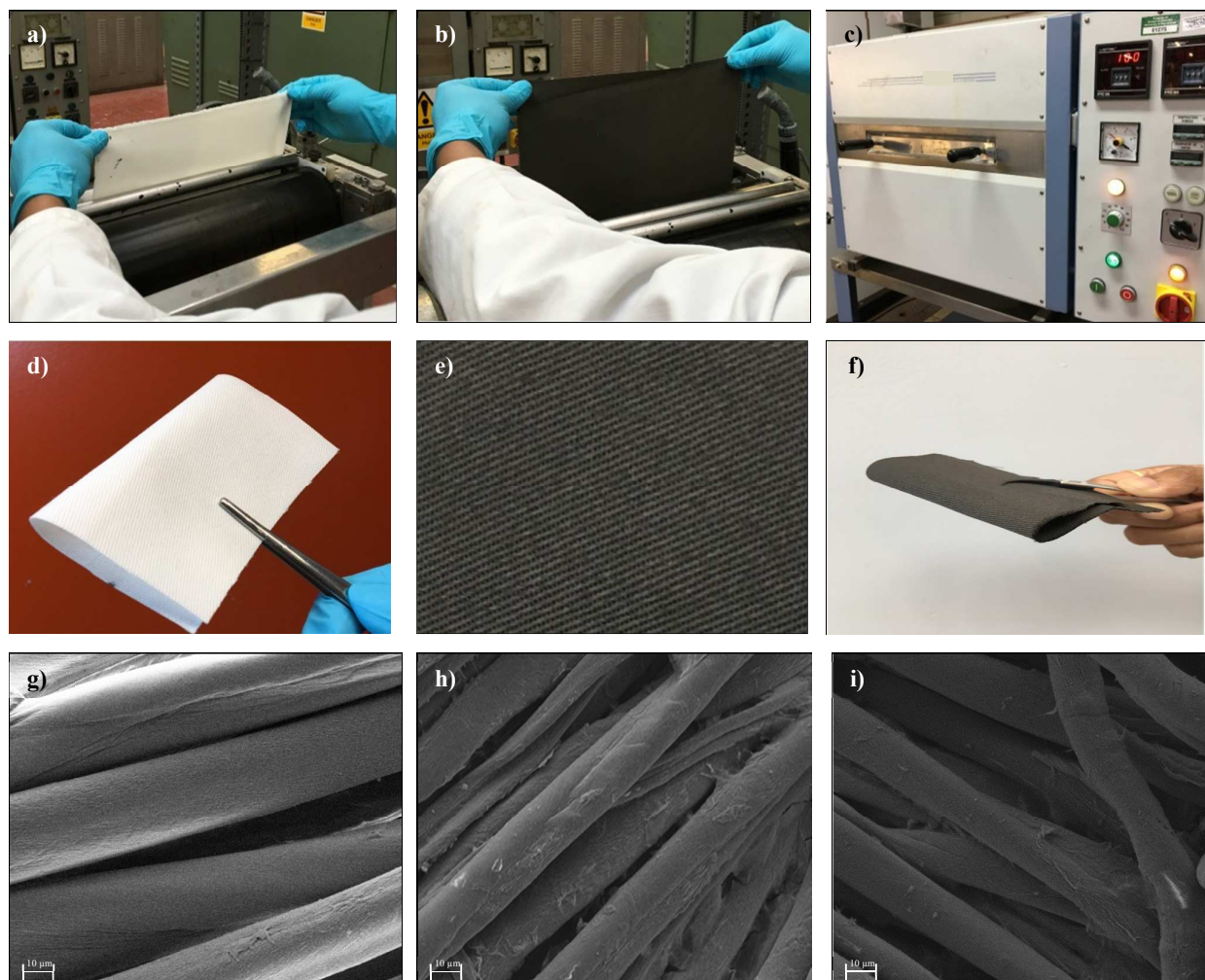


**Figure 3.** a) Untreated cotton fabric was passed through padding bath and rollers; b) rGO coated cotton fabric immediately after padding; c) Drying of rGO coated cotton fabric at 100 °C for 5 mins; d) Untreated control cotton fabric; e) rGO coated cotton fabric after 5 padding pass and drying; f) Demonstration of flexibility and drape of rGO coated cotton fabric; g) SEM image of untreated control cotton fabrics (X1000); h) SEM image of rGO coated cotton fabric (X1000); and i) SEM image of washed (5 times) rGO coated cotton fabric (X1000).

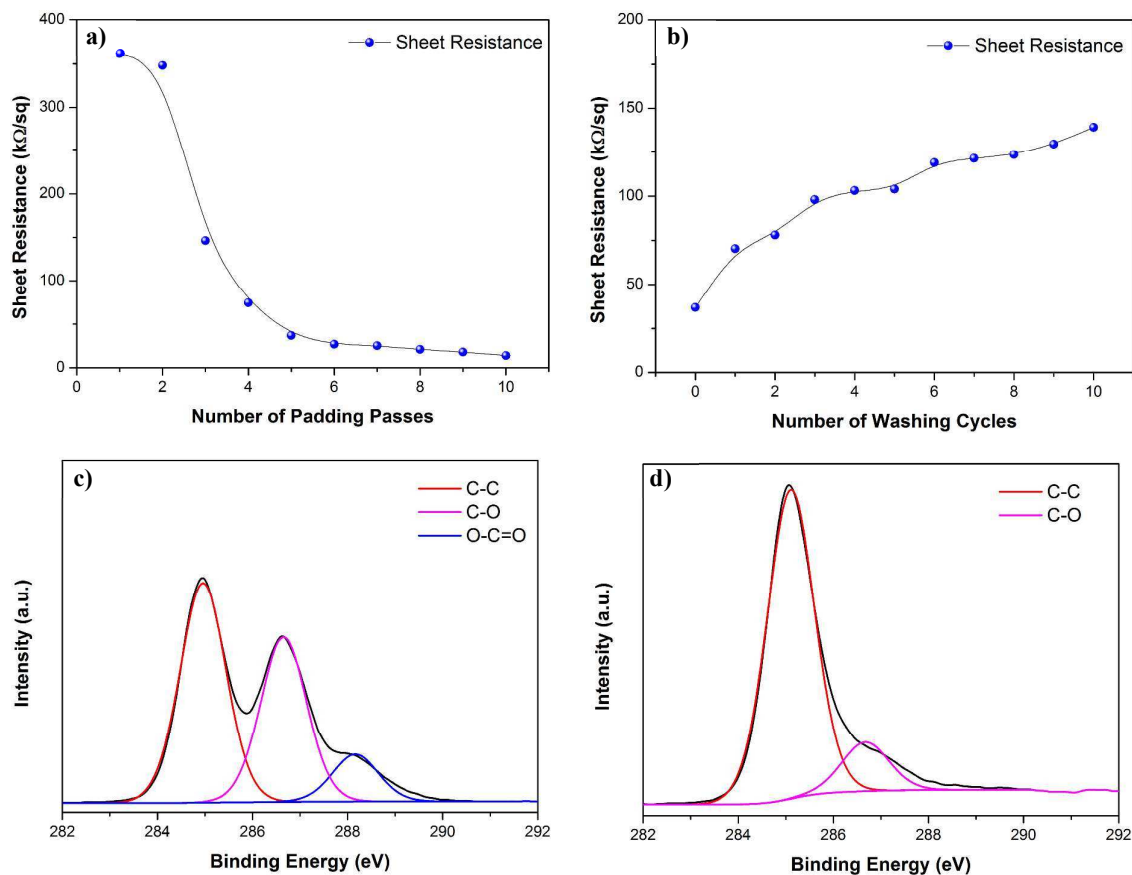


**Figure 4.** a) Sheet resistance Vs Number of padding passes; b) The change of sheet resistance with number of washing cycles; c) High resolution C (1s) XPS spectrum of control cotton fabric; d) High resolution C (1s) XPS spectrum of rGO padded cotton fabric;

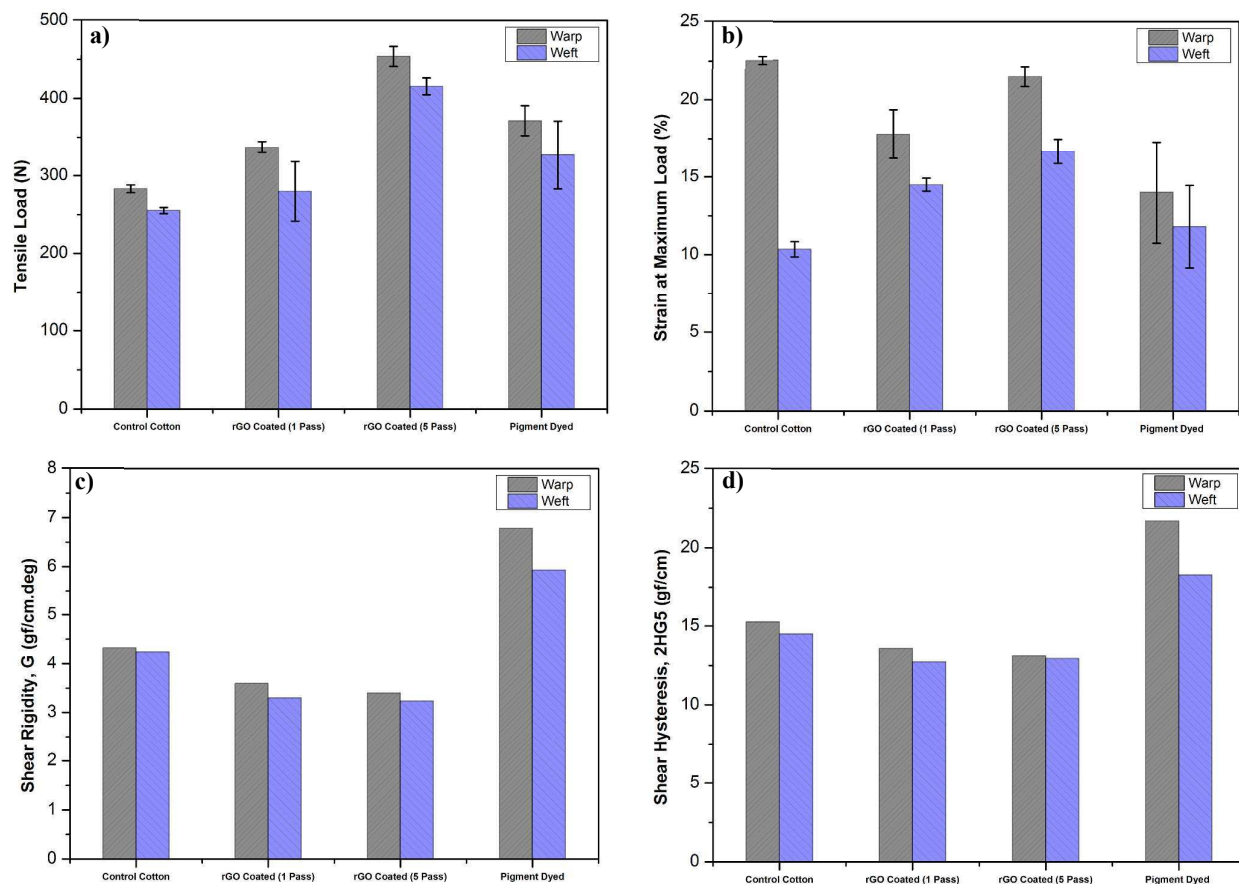


**Figure 5.** Effect of rGO coatings and pigment dyeing on a) Tensile strength at maximum load and b) Strain% at maximum load; c) Shear rigidity, G and d) Shear hysteresis at  $5^\circ$ , 2HG5 of cotton fabrics

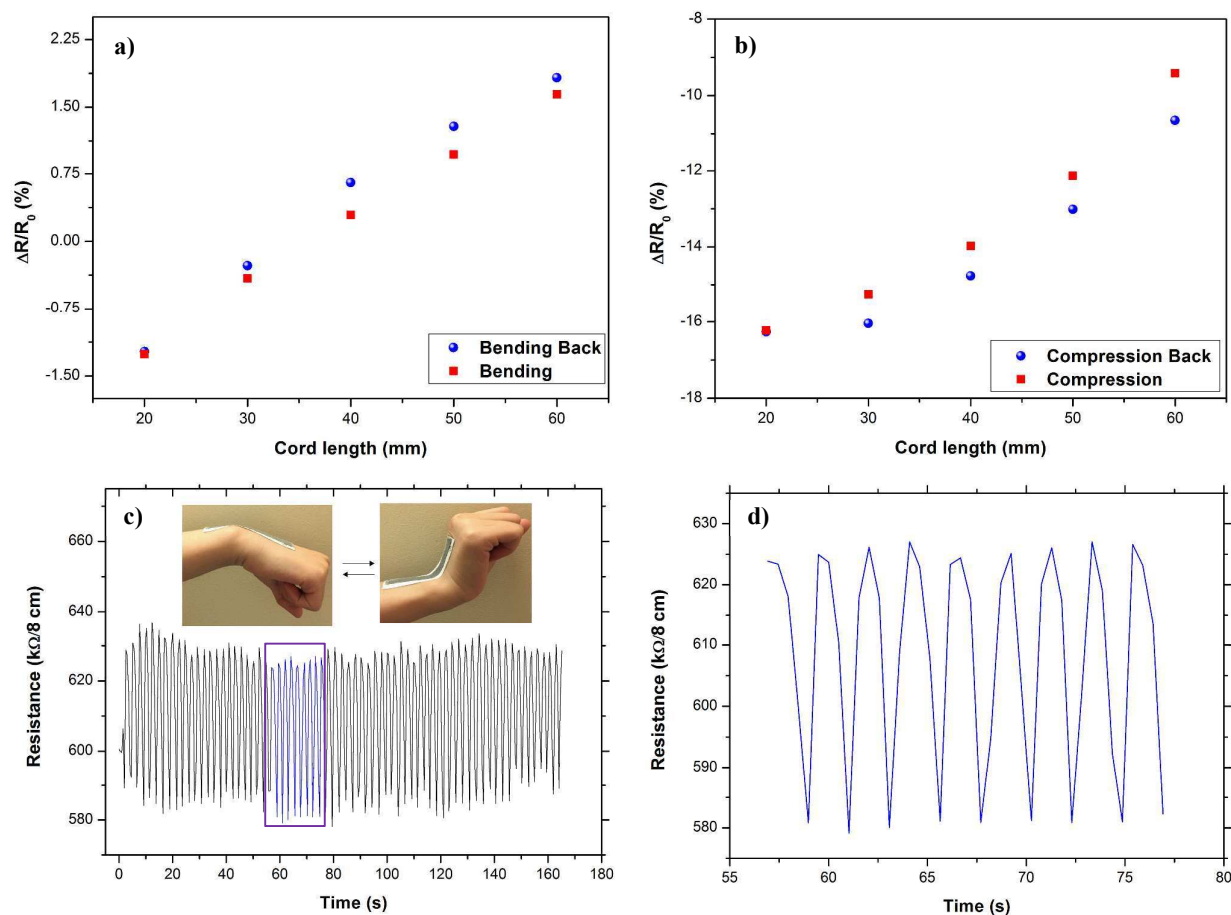


**Figure 6.** a) The variation in resistance of the bending sensor in forward (bending) and reverse (bending back) direction; b) The variation in resistance of the compression sensor in forward (compression) and reverse (compression back) direction; c) The upward and downward movement of rGO coated cotton fabric mounted on a wrist joint; d) Expanded version of purple box in Figure 6(c) from 57s to 77s;

### Table of contents (TOC) figure

A simple, scalable and cost-effective method of producing graphene-based wearable e-textiles is reported. This could potentially manufacture conductive graphene e-textiles at commercial production rates of  $\sim 150$  m/min.

